

I. Comez · M. A. Guler

# The contact problem of a rigid punch sliding over a functionally graded bilayer

Received: 21 September 2016 / Revised: 5 February 2017 / Published online: 11 March 2017  
© Springer-Verlag Wien 2017

**Abstract** In this study, the plane contact problem for a rigid cylindrical punch and a functionally graded bilayer is considered. The layers have different thicknesses and elastic constants. The normal and tangential forces are applied to the upper layer with a rigid cylindrical punch, and the lower layer is fully bonded to a rigid substrate. Poisson's ratios are taken as constant, and elasticity moduli are assumed to vary exponentially through the thickness of the layers. With the use of Fourier integral transform, the plane contact problem is reduced to a singular integral equation in which the unknowns are the contact pressure and the contact width. The singular integral equation is solved numerically using Gauss–Jacobi integration formula. The effect of several geometrical and physical parameters such as the material inhomogeneity, the friction coefficient, the layers' height, the mismatch in the material properties at the interface, and the contact width on the contact stress and in-plane stress are investigated in detail.

## 1 Introduction

Functionally graded materials (FGMs) are relatively novel multi-functional materials, which are made up of a mixture of disparate materials, such as ceramics and metals with gradual variation in the mechanical properties with position. The volume fractions of the constituent materials can be arranged so that there is smooth and continuous gradual variation using various manufacturing methods, such as powder metallurgy, vapor deposition techniques, centrifugal methods, and solid free-form methods [19].

The studies in the contact mechanics pertaining to FGMs are mostly related to the contact problems of functionally graded (FG) layers or FG half planes. The contact problem of an FG half plane was studied by Bakirtas [2], Giannakopoulos and Suresh [12, 13], Giannakopoulos and Pallot [11], Dag et al. [9], Chen et al. [4], and Guler et al. [16]. Giannakopoulos and Suresh [12, 13] treated the axisymmetric contact problem both analytically and computationally when the medium is subjected to a point force or a rigid indenter. The plane contact problem was treated when the elastic modulus is assumed to vary exponentially in depth direction [2], according to a power law variation [11], in an exponential form either in the lateral direction [9], in the thickness direction [16] or in an arbitrary direction [4].

The plane strain contact problems of a single FG layer bonded to a rigid substrate or Winkler foundation are studied by Choi [6] and Comez [7, 8]. The FG layer is loaded by a frictional sliding flat punch [6] and by a frictionless rigid cylindrical punch [7]. The moving contact problem for an FG layer was studied by Comez [8].

---

I. Comez (✉)  
Department of Civil Engineering, Karadeniz Technical University, 61080 Trabzon, Turkey  
E-mail: isacomez@hotmail.com

M. A. Guler  
Department of Mechanical Engineering, TOBB University of Economics and Technology, 06560 Söğütözü, Ankara, Turkey

Contact problems involving the graded coatings bonded to a homogeneous substrate are widely considered by several researchers. The frictional sliding contact problem of a graded coating bonded to a homogeneous substrate is solved under plane strain-state assumption by Guler and Erdogan [14, 15], Ke and Wang [18], and Chen and Chen [3], and by Alinia et al. [1] using Fourier integral transform techniques. Guler and Erdogan [14, 15] and Alinia et al. [1] studied the frictional sliding contact problems analytically where the loading was provided by a sliding rigid stamp whose profile can be flat, triangular, cylindrical or semicircular by assuming an exponential variation in the elastic modulus. A multilayered model for the frictional sliding contact problem with arbitrarily varying elastic modulus is investigated by Ke and Wang [18]. The elastic modulus is assumed to vary according to a linear law in Chen and Chen [3]. The axisymmetric frictionless contact of the graded coatings with arbitrary spatial variations of elastic modulus bonded to a homogeneous substrate is investigated by Ke and Wang [17] and Liu et al. [20] using Hankel integral transform technique. The frictionless and frictional contact problems of a homogeneous coating-graded interlayer-substrate structure are considered by Yang and Ke [22] and Chidlow and Teodorescu [5]. Miranda et al. [21] studied the contact-induced transverse fracture modes in trilayers consisting of brittle bilayer coating on soft substrates, and they calculated the critical loads for radial cracking with the finite element method.

Although there are many studies in the literature that deal with a graded coating perfectly bonded to a homogeneous half plane, the sliding frictional contact problem between a rigid circular punch and a graded bilayer is not considered in the open literature. In this study, the contact problem of an FG coating bonded to a homogeneous substrate is extended to the contact problem of a graded bilayer in the presence of friction. The normal and tangential forces are applied to the upper layer with a rigid cylindrical punch, and the lower layer is fully bonded to a rigid substrate. Poisson's ratios are taken as constant, and the elasticity moduli are assumed to vary exponentially through the thickness of the layers. With the use of Fourier integral transform, the plane contact problem is reduced to a singular integral equation in which the unknowns are the contact pressure and the contact width. The singular integral equation is solved numerically using Gauss–Jacobi integration formula. The effect of the material inhomogeneity, the coefficient of friction, the height of the layers, mismatch in the shear modulus at the interface, and contact width on the contact pressure and the in-plane stress is examined in detail.

## 2 Formulation of the problem

Consider the frictional plane strain contact problem shown in Fig. 1. A rigid cylindrical punch with radius  $R$  transmits a concentrated normal force  $P$  and a tangential force  $Q(=\eta P)$  to the upper FG elastic layer of thickness  $h_2$ . The FG layers are fully bonded to each other, and the lower FG layer of thickness  $h_2$  is supported by a rigid foundation. Poisson's ratios  $\nu_i$  ( $i = 1, 2$ ) are taken as constants, and the shear moduli  $\mu_i$  ( $i = 1, 2$ ) are assumed to vary exponentially through the thickness of the layers as follows:

$$\mu_1(y) = \mu_{10}e^{\gamma_1 y}, \quad -h_1 \leq y \leq 0, \quad (1.1)$$

$$\mu_2(y) = \mu_{20}e^{\gamma_2 y}, \quad -h \leq y \leq -h_1 \quad (1.2)$$

where  $\mu_{10}$  and  $\mu_{20}$  are the shear moduli defined at the top surface ( $y = 0$ ) of the graded bilayer, and  $\gamma_i$  ( $i = 1, 2$ ) is the inhomogeneity parameter controlling the variation of the shear modulus for the corresponding  $i$ 'th graded layer. The subscript  $i$  denotes the related layer, that is, the subscripts 1 and 2 refer to the upper and lower layers, respectively.

Defining

$$\Gamma_1 = \frac{\mu_{11}}{\mu_{10}} = e^{-\gamma_1 h_1}, \quad (2.1)$$

$$\Gamma_2 = \frac{\mu_{22}}{\mu_{21}} = e^{-\gamma_2 h_2}, \quad (2.2)$$

$$\Gamma_0 = \frac{\mu_{21}}{\mu_{11}} = \frac{\mu_{20}e^{-\gamma_2 h_1}}{\mu_{10}e^{-\gamma_1 h_1}}, \quad (2.3)$$

the inhomogeneity parameter may be expressed as:

$$\gamma_i h_i = -\log \Gamma_i, \quad i = 1, 2 \quad (3)$$

where  $\Gamma_0$  is the parameter defining the mismatch in the shear modulus at the interface of the layers.

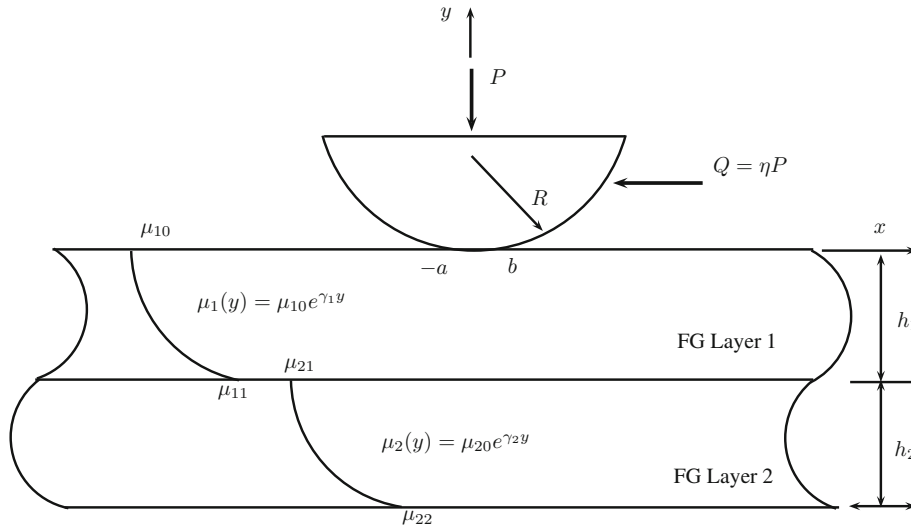


Fig. 1 Geometry of the problem

Assuming that the functionally graded layers are isotropic, for the plane strain contact problem Hooke’s law can be written as follows:

$$\sigma_{xi}(x, y) = \frac{\mu_i(y)}{\kappa_i - 1} \left[ (\kappa_i + 1) \frac{\partial u_i}{\partial x} + (3 - \kappa_i) \frac{\partial v_i}{\partial y} \right], \quad i = 1, 2, \tag{4.1}$$

$$\sigma_{yi}(x, y) = \frac{\mu_i(y)}{\kappa_i - 1} \left[ (3 - \kappa_i) \frac{\partial u_i}{\partial x} + (\kappa_i + 1) \frac{\partial v_i}{\partial y} \right], \quad i = 1, 2, \tag{4.2}$$

$$\tau_{xyi} = \mu_i(y) \left[ \frac{\partial u_i}{\partial y} + \frac{\partial v_i}{\partial x} \right], \quad i = 1, 2 \tag{4.3}$$

where  $u_i, v_i$  are the  $x$ - and  $y$ -components of the displacement vector.

Substituting Eq. (4) into the equilibrium equations, Navier’s equations in terms of the  $u_i(x, y)$  and  $v_i(x, y)$  can be obtained as follows:

$$\begin{aligned} (\kappa_i + 1) \frac{\partial^2 u_i}{\partial x^2} + (\kappa_i - 1) \frac{\partial^2 u_i}{\partial y^2} + 2 \frac{\partial^2 v_i}{\partial x \partial y} \\ + 2\gamma_i(\kappa_i - 1) \left[ \frac{\partial u_i}{\partial y} + \frac{\partial v_i}{\partial x} \right] = 0, \quad i = 1, 2, \end{aligned} \tag{5.1}$$

$$\begin{aligned} (\kappa_i - 1) \frac{\partial^2 v_i}{\partial x^2} + (\kappa_i + 1) \frac{\partial^2 v_i}{\partial y^2} + 2 \frac{\partial^2 u_i}{\partial x \partial y} \\ + \gamma_i \left[ (3 - \kappa_i) \frac{\partial u_i}{\partial x} + (\kappa_i + 1) \frac{\partial v_i}{\partial y} \right] = 0. \quad i = 1, 2. \end{aligned} \tag{5.2}$$

By using the Fourier transforms, the displacement components may be written as:

$$u_i(x, y) = \frac{1}{2\pi} \int_{-\infty}^{\infty} \tilde{u}_i(\alpha, y) e^{-I\alpha x} d\alpha, \quad i = 1, 2, \tag{6.1}$$

$$v_i(x, y) = \frac{1}{2\pi} \int_{-\infty}^{\infty} \tilde{v}_i(\alpha, y) e^{-I\alpha x} d\alpha, \quad i = 1, 2 \tag{6.2}$$

where  $\tilde{u}_i(\alpha, y)$  and  $\tilde{v}_i(\alpha, y)$  are Fourier transforms of  $u_i(x, y)$  and  $v_i(x, y)$ , respectively, and  $I = \sqrt{-1}$ .

Substituting Eq. (6) into Eq. (5), the following ordinary differential equations are obtained:

$$\begin{aligned}
 &(\kappa_i - 1) \frac{d^2 \tilde{u}_i}{dy^2} - 2I\alpha \frac{d\tilde{v}_i}{dy} - \alpha^2(\kappa_i + 1)\tilde{u}_i \\
 &+ \gamma_i(\kappa_i - 1) \left( \frac{d\tilde{u}_i}{dy} - I\alpha \tilde{v}_i \right) = 0, \quad i = 1, 2,
 \end{aligned} \tag{7.1}$$

$$\begin{aligned}
 &(\kappa_i + 1) \frac{\partial^2 \tilde{v}_i}{\partial y^2} - 2I\alpha \frac{\partial \tilde{u}_i}{\partial y} - \alpha^2(\kappa_i - 1) \tilde{v}_i \\
 &+ \gamma_i(\kappa_i + 1) \left( \frac{\partial \tilde{v}_i}{\partial y} - I\alpha \frac{3 - \kappa_i}{\kappa_i + 1} \right) \tilde{v}_i = 0. \quad i = 1, 2.
 \end{aligned} \tag{7.2}$$

Equation (7) can be solved for  $\tilde{u}_i, \tilde{v}_i$ , and the following associated characteristic polynomial may be obtained:

$$n_i^4 + 2\gamma_i n_i^3 + (\gamma_i^2 - 2\alpha^2)n_i^2 - 2\alpha^2\gamma_i n_i + \alpha^2 \left( \alpha^2 + \gamma_i^2 \frac{3 - \kappa_i}{\kappa_i + 1} \right) = 0, \tag{8}$$

The roots of the characteristic Eq. (8) are given by

$$n_{i1} = -\frac{1}{2} \left( \gamma_i + \sqrt{4\alpha^2 + \gamma_i^2 + 4I|\alpha||\gamma_i| \sqrt{\frac{3 - \kappa_i}{\kappa_i + 1}}} \right), \quad i = 1, 2, \tag{9.1}$$

$$n_{i2} = -\frac{1}{2} \left( \gamma_i + \sqrt{4\alpha^2 + \gamma_i^2 - 4I|\alpha||\gamma_i| \sqrt{\frac{3 - \kappa_i}{\kappa_i + 1}}} \right), \quad i = 1, 2, \tag{9.2}$$

$$n_{i3} = -\frac{1}{2} \left( \gamma_i - \sqrt{4\alpha^2 + \gamma_i^2 + 4I|\alpha||\gamma_i| \sqrt{\frac{3 - \kappa_i}{\kappa_i + 1}}} \right), \quad i = 1, 2, \tag{9.3}$$

$$n_{i4} = -\frac{1}{2} \left( \gamma_i - \sqrt{4\alpha^2 + \gamma_i^2 - 4I|\alpha||\gamma_i| \sqrt{\frac{3 - \kappa_i}{\kappa_i + 1}}} \right). \quad i = 1, 2. \tag{9.4}$$

The solution of Eq. (7) can be obtained in terms of the roots of the characteristic equation as follows:

$$\tilde{u}_i(y) = \sum_{j=1}^4 A_{ij} e^{n_{ij}y}, \quad i = 1, 2, \tag{10.1}$$

$$\tilde{v}_i(y) = -I \sum_{j=1}^4 A_{ij} m_{ij} e^{n_{ij}y}. \quad i = 1, 2 \tag{10.2}$$

where

$$m_{ij} = \frac{[2n_{ij} + \gamma_i(3 - \kappa_i)] \left[ n_{ij}^2(1 + \kappa_i) + n_{ij}\gamma_i(1 + \kappa_i) - \alpha^2(3 + \kappa_i) \right]}{\alpha [4\alpha^2 + \gamma_i^2(3 - \kappa_i)(1 + \kappa_i)]}, \tag{11}$$

$i = 1, 2, \quad j = 1, \dots, 4.$

Substituting Eqs. (9–11) into Eq. (6) and further substituting into Eq. (4), the stress components for the layers are readily obtained as

$$\sigma_{xi}(x, y) = \frac{1}{2\pi} I \int_{-\infty}^{\infty} \frac{\mu_i(y)}{\kappa_i - 1} \sum_{j=1}^4 A_{ij} [(\kappa_i - 3)m_{ij}n_{ij} - \alpha(\kappa_i + 1)] e^{n_{ij}y} e^{-I\alpha x} d\alpha, \tag{12.1}$$

$$\sigma_{y_i}(x, y) = \frac{1}{2\pi} I \int_{-\infty}^{\infty} \frac{\mu_i(y)}{\kappa_i - 1} \sum_{j=1}^4 A_{ij} [\alpha(\kappa_i - 3) - (\kappa_i + 1)m_{ij}n_{ij}] e^{n_{ij}y} e^{-I\alpha x} d\alpha, \tag{12.2}$$

$$\tau_{x_{y_i}}(x, y) = \frac{1}{2\pi} \int_{-\infty}^{\infty} \sum_{j=1}^4 \mu_i(y) A_{ij} [(n_{ij} - \alpha m_{ij})] e^{n_{ij}y} e^{-I\alpha x} d\alpha \tag{12.3}$$

where  $A_{ij}$  are the unknowns, which will be determined from the boundary conditions of the problem.

### 3 The boundary conditions and the singular integral equation

The plane contact problem outlined above is subjected to the following boundary conditions:

$$\sigma_{y1}(x, 0) = \begin{cases} -p(x), & -a < x < b \\ 0, & x \leq a, x \geq b, \end{cases} \tag{13.1}$$

$$\tau_{xy1}(x, 0) = \begin{cases} -\eta p(x), & -a < x < b \\ 0, & x \leq a, x \geq b, \end{cases} \tag{13.2}$$

$$\sigma_{y1}(x, -h_1) = \sigma_{y2}(x, -h_1) \quad (-\infty \leq x < \infty), \tag{13.3}$$

$$\tau_{xy1}(x, -h_1) = \tau_{xy2}(x, -h_1) \quad (-\infty \leq x < \infty), \tag{13.4}$$

$$u_1(x, -h_1) = u_2(x, -h_1) \quad (-\infty \leq x < \infty), \tag{13.5}$$

$$v_1(x, -h_1) = v_2(x, -h_1) \quad (-\infty \leq x < \infty), \tag{13.6}$$

$$u_2(x, -h) = 0 \quad (-\infty \leq x < \infty), \tag{13.7}$$

$$v_2(x, -h) = 0 \quad (-\infty \leq x < \infty) \tag{13.8}$$

where  $p(x)$  is the a priori unknown contact pressure between the rigid punch and the layer on the contact area  $(-a, b)$ . By using the boundary conditions (13), eight of the unknown functions  $A_{ij}$  appearing in Eq. (10) may be obtained in terms of the unknown function  $p(x)$  as follows:

$$A_{ij} = \frac{1}{\mu_{10}} \int_{-a}^b p(t) e^{I\alpha t} (A_{ij}^p + \eta A_{ij}^q) dt, \tag{14}$$

The unknown contact pressure  $p(x)$  is determined from the following mixed condition:

$$\frac{\partial v_1(x, 0)}{\partial x} = \frac{x}{R} \quad -a < x < b. \tag{15}$$

Condition (15) gives the following singular integral equation:

$$\eta \frac{\phi_2}{\phi_1} p(x) + \frac{1}{\pi} \int_{-a}^b p(t) \left[ \frac{1}{t-x} + k(x, t) \right] dt = \frac{\mu_{10}}{\phi_1} \frac{x}{R} \tag{16}$$

where

$$k(x, t) = k_1(x, t) + \eta k_2(x, t), \tag{17.1}$$

$$k_1(x, t) = \frac{1}{\phi_1} \int_0^{\infty} (M_1(\alpha) - \phi_1) \sin \alpha(t-x) d\alpha, \tag{17.2}$$

$$k_2(x, t) = \frac{1}{\phi_1} \int_0^{\infty} (M_2(\alpha) - \phi_2) \cos \alpha(t-x) d\alpha, \tag{17.3}$$

$$M_1(\alpha) = -I\alpha \sum_{j=1}^4 A_{1j}^p m_{1j}, \tag{17.4}$$

$$M_2(\alpha) = -\alpha \sum_{j=1}^4 A_{1j}^q m_{1j}, \tag{17.5}$$

$$\phi_1 = \lim_{\alpha \rightarrow \infty} M_1(\alpha) = -\frac{\kappa_1 + 1}{4}, \tag{17.6}$$

$$\phi_2 = \lim_{\alpha \rightarrow \infty} M_2(\alpha) = \frac{\kappa_1 - 1}{4}. \tag{17.7}$$

In the singular integral equation (16), the contact areas  $a$  and  $b$  are also unknown a priori, as well as the contact pressure  $p(x)$ . To complete the solution of the problem, the contact stress  $p(x)$  must satisfy the following equilibrium condition:

$$\int_{-a}^b p(t)dt = P. \tag{18}$$

**4 On the solution of the singular integral equation**

Because of the smooth contact at the end points  $x = -a, x = b$ , the physics of the problem requires that the index of the integral equation (16) is  $-1$  [10]. Applying the following transformations:

$$t = \frac{a+b}{2}r + \frac{b-a}{2}, \quad x = \frac{a+b}{2}s + \frac{b-a}{2}, \tag{19.1}$$

$$\alpha = z/R, \quad \varphi(r) = \frac{p(r)}{\mu_{10}} \tag{19.2}$$

the integral equation (16) and the equilibrium condition (18) may be expressed in the following form:

$$\eta \frac{\phi_2}{\phi_1} \varphi(s) + \frac{1}{\pi} \int_{-1}^1 \varphi(r) \left[ \frac{1}{r-s} + \frac{a+b}{2R} k(s,r) \right] dr = \frac{1}{\phi_1} \left( \frac{a+b}{2R} s + \frac{b-a}{2R} \right), \tag{20}$$

$$\frac{a+b}{2R} \int_{-1}^1 \varphi(r) dr = \frac{P}{\mu_{10}R}. \tag{21}$$

The solution of the integral equation can be expressed as:

$$\varphi(r) = g(r)w(r) \tag{22}$$

where  $g(r)$  is a continuous and bounded function in the interval  $[-1, 1]$ .  $w(r)$  is the weight function related to Jacobi polynomial,

$$w(r) = (1-r)^\alpha (1+r)^\beta, \tag{23.1}$$

$$\alpha = \frac{1}{2\pi i} \ln \left[ \frac{\eta \frac{\phi_2}{\phi_1} - I}{\eta \frac{\phi_2}{\phi_1} + I} \right] + N_0, \tag{23.2}$$

$$\beta = -\frac{1}{2\pi i} \ln \left[ \frac{\eta \frac{\phi_2}{\phi_1} - I}{\eta \frac{\phi_2}{\phi_1} + I} \right] + M_0 \tag{23.3}$$

where  $N_0$  and  $M_0$  are arbitrary (positive, zero, or negative) integers and must be determined considering  $0 < \text{Re}[\alpha, \beta] < 1$  for the index  $-1$ . By using Gauss–Jacobi integration formulas, the integral equation (20) can be converted to the equivalent system of algebraic equations as follows [10]:

$$\sum_{\xi=1}^N W_{\xi}^N \left[ \frac{1}{r_{\xi} - s_k} + \frac{a+b}{2R} k(s_k, r_{\xi}) \right] g(r_{\xi}) = \frac{1}{\phi_1} \left( \frac{a+b}{2R} s_k + \frac{b-a}{2R} \right),$$

$$k = 1, \dots, N + 1 \tag{24}$$

where  $r_i$  and  $s_k$  are the roots of the related Jacobi polynomials and  $W_{\xi}^N$  is the weighting constant:

$$P_N^{(\alpha, \beta)}(r_{\xi}) = 0, \quad \xi = 1, 2, \dots, N, \tag{25.1}$$

$$P_{N+1}^{(-\alpha, -\beta)}(s_k) = 0, \quad k = 1, 2, \dots, N + 1, \tag{25.2}$$

$$W_{\xi}^N = -\frac{1}{\pi} \frac{(2N + \alpha + \beta + 2) \Gamma(\alpha + N + 1) \Gamma(\beta + N + 1)}{(N + 1)! \Gamma(N + \alpha + \beta + 1)} \frac{2^{(\alpha + \beta)}}{P_N^{(\alpha, \beta)}(r_{\xi}) P_{N+1}^{(-\alpha, -\beta)}(r_{\xi})}. \tag{25.3}$$

For a given value of the contact width  $(a + b)/R$ , Eq (25) gives  $N + 1$  equations to determine the  $N + 1$  unknowns, which are  $g(r_{\xi})$  and  $(b - a)/R$ . Note that there are  $N + 1$  equations to determine the  $N$  unknowns

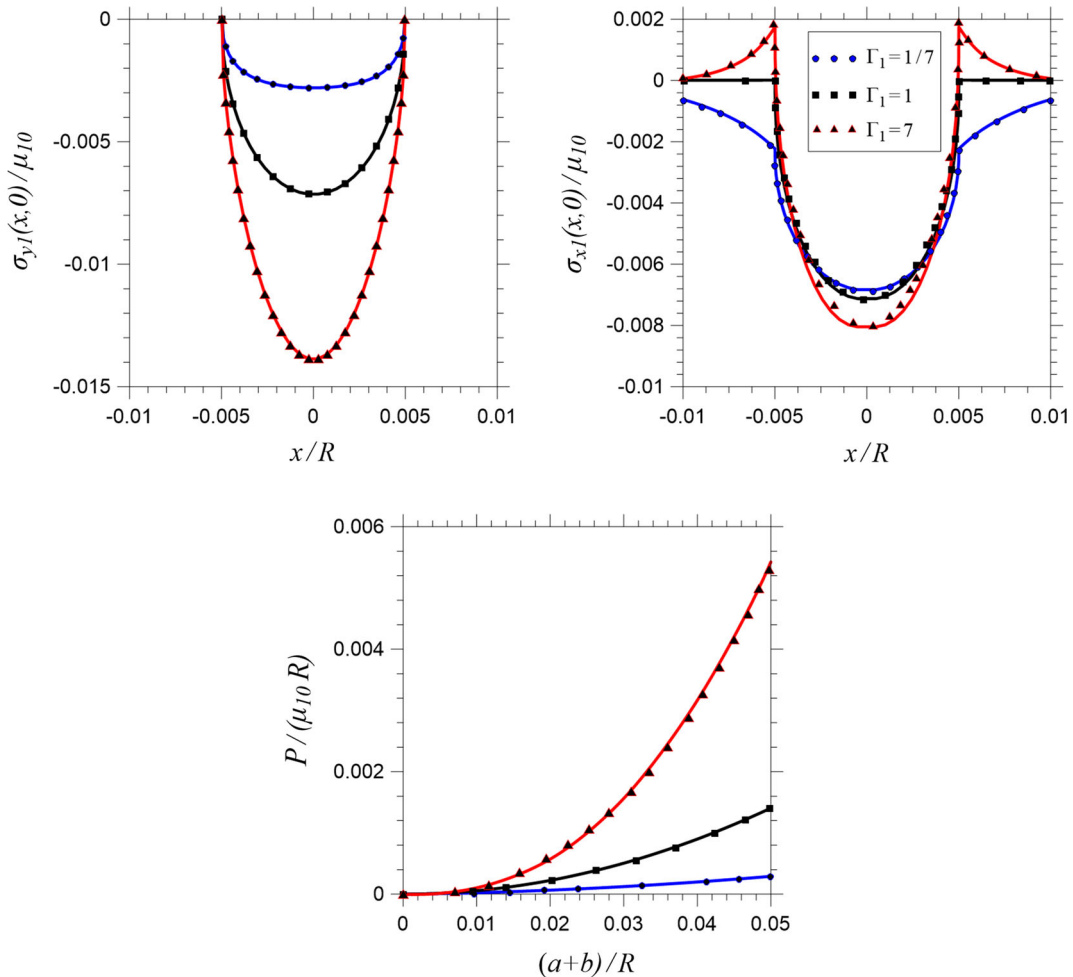


**Fig. 2** Comparison of the stress distribution on the surface of the FGM layers with that of Guler and Erdogan [15]; the *solid curves* present the current and the *symbols* present Guler and Erdogan [15] solution. ( $\eta = 0, \Gamma_1 = \mu_{11}/\mu_{10}, \Gamma_2 = \mu_{22}/\mu_{21} = 1, R/h_1 = 100, (a + b)/R = 0.01, h_2/h_1 \rightarrow \infty$ )

$g(r_\xi)$  in Eq. (25). The additional equation (provided by  $s_1, \dots, s_{N+1}$ ) is equivalent to the consistency condition of the integral equation, and an equation corresponding to one of the  $s_k$  is extracted from (24) to determine the eccentricity parameter  $(b - a)/R$ . The system of equations is linear in terms of the  $g(r_\xi)$  but highly nonlinear in variable  $(b - a)/R$ . Therefore, an iterative method is used to obtain the unknowns. Note that in the frictionless case it is no need to iteration because the eccentricity parameter is zero, and the  $(N/2 + 1)$ -th equation in (25) is automatically satisfied. Once Eq. (25) is solved, the dimensionless load parameter can be calculated from the equilibrium condition (21) as

$$\frac{P}{\mu_{10}R} = \pi \frac{a + b}{2R} \sum_{\xi=1}^N W_\xi^N g(r_\xi). \tag{26}$$

The surface stress components in dimensionless form can be computed using the following relations:

$$\frac{\sigma_{y1}(x, 0)}{\mu_{10}} = -\frac{p(x)}{\mu_{10}}, \tag{27}$$

$$\frac{\tau_{xy1}(x, 0)}{\mu_{10}} = -\eta \frac{p(x)}{\mu_{10}}, \tag{28}$$

$$\frac{\sigma_{x1}(x, 0)}{\mu_{10}} = \begin{cases} \phi_3 p(x)/\mu_{10} + H(x), & -a < x < b \\ H(x), & x \leq -a, x \geq b \end{cases} \tag{29}$$

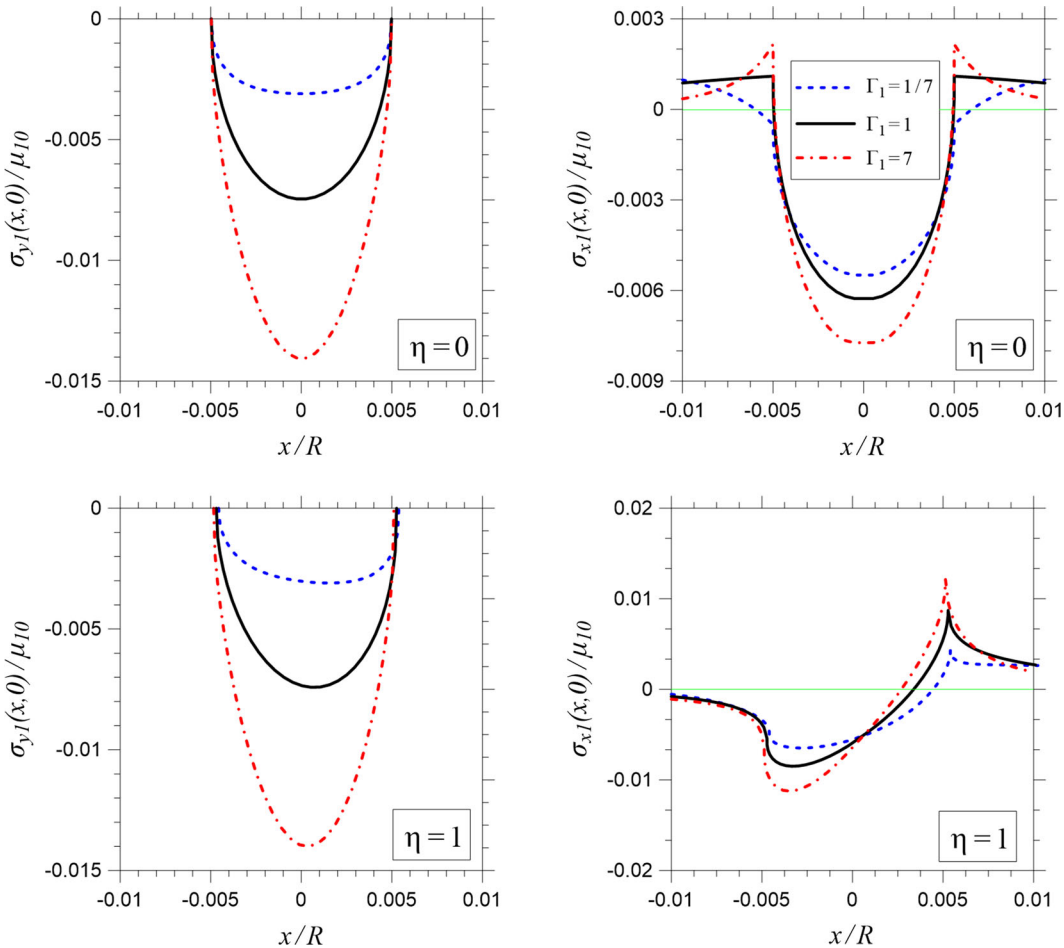


**Fig. 3** Contact stress and in-plane stress distribution for various values of the stiffness ratio,  $\Gamma_1 = \mu_{11}/\mu_{10}$ ,  $\Gamma_2 = \mu_{22}/\mu_{21} = 1$ ,  $R/h_1 = 100$ ,  $(a + b)/R = 0.01$ ,  $h_2/h_1 = 1$



where

$$H(x) = \frac{1}{\pi\mu_{10}} \int_{-a}^b p(t) \left[ \phi_4 \frac{\eta}{t-x} + k_3(x, t) + \eta k_4(x, t) \right] dt, \tag{30.1}$$

$$k_3(x, t) = \int_0^\infty (M_3(\alpha) - \phi_3) \cos \alpha(t-x) d\alpha, \tag{30.2}$$

$$k_4(x, t) = \int_0^\infty (M_4(\alpha) - \phi_4) \sin \alpha(t-x) d\alpha, \tag{30.3}$$

$$M_3(\alpha) = I \frac{1}{\kappa_1 - 1} \sum_{j=1}^4 A_{1j}^p [(\kappa_1 - 3)m_{1j}n_{1j} - \alpha(\kappa_1 + 1)], \tag{30.4}$$

$$M_4(\alpha) = -\frac{1}{\kappa_1 - 1} \sum_{j=1}^4 A_{1j}^q [(\kappa_1 - 3)m_{1j}n_{1j} - \alpha(\kappa_1 + 1)], \tag{30.5}$$

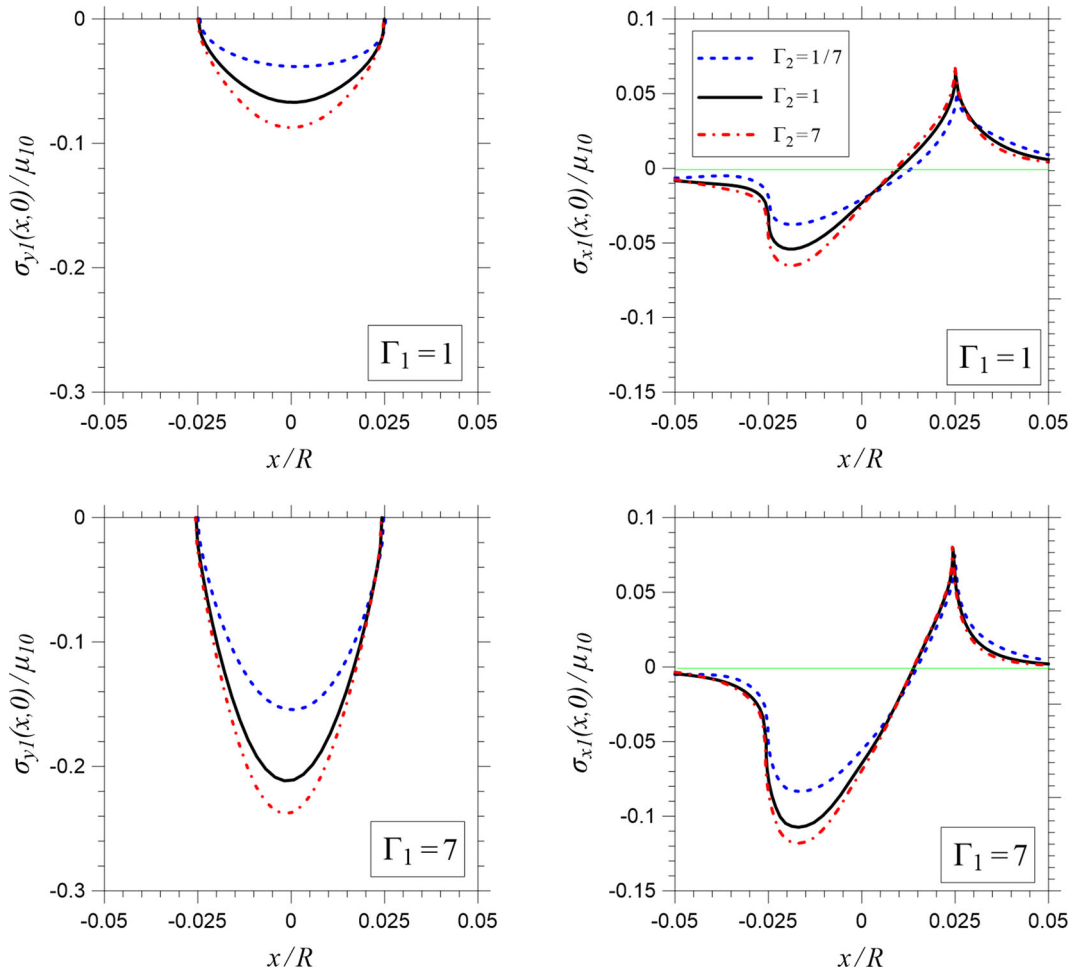


**Fig. 4** Contact stress and in-plane stress distribution for various values of the stiffness ratio,  $\Gamma_2 = \mu_{22}/\mu_{21}$ ,  $\Gamma_1 = \mu_{11}/\mu_{10}$ ,  $\eta = 0.5$ ,  $R/h_1 = 100$ ,  $(a + b)/R = 0.05$ ,  $h_2/h_1 = 1$

$$\phi_3 = \lim_{\alpha \rightarrow \infty} M_3(\alpha) = -1, \tag{30.6}$$

$$\phi_4 = \lim_{\alpha \rightarrow \infty} M_4(\alpha) = -2. \tag{30.7}$$

### 5 Numerical results and discussion

In this study, the plane frictional contact problem between a rigid cylindrical punch and an FG bilayer, is investigated. The main quantities of interest are the contact stress, the in-plane stress component on the surface of the FG bilayer, and the load versus contact width for various material and geometrical parameters such as the stiffness ratios,  $\Gamma_1, \Gamma_2$ , the friction coefficient,  $\eta$ , the thickness ratio,  $h_1/h_2$ , the stiffness discontinuity at the interface,  $\Gamma_0$ , and the contact width,  $(a + b)/R$ . Poisson’s ratios of the FG bilayers are assumed to be constant,  $\nu_1 = \nu_2 = 0.3$ , and unless otherwise stated, the stiffness discontinuity at the interface,  $\Gamma_0$ , is taken to be unity in the following analysis.

The results of the current study can be validated with those of Guler and Erdogan [15] by letting  $h_2 \rightarrow \infty$  and  $\Gamma_2 = 1$ . Figure 2 shows an excellent match in the validation results in terms of contact pressure and in-plane stress distribution as well as load versus the contact length results.

The distributions of normalized contact pressure  $\sigma_{y1}(x, 0)/\mu_{10}$  and normalized in-plane surface stress component  $\sigma_{x1}(x, 0)/\mu_{10}$  are plotted for various values of the stiffness ratio,  $\Gamma_1 = \mu_{11}/\mu_{10}$  by taking  $\Gamma_2 = \mu_{22}/\mu_{21} = 1, R/h_1 = 100, (a + b)/R = 0.01, h_2/h_1 = 1$  in Fig. 3. Note that Fig. 3a, b is for the frictionless

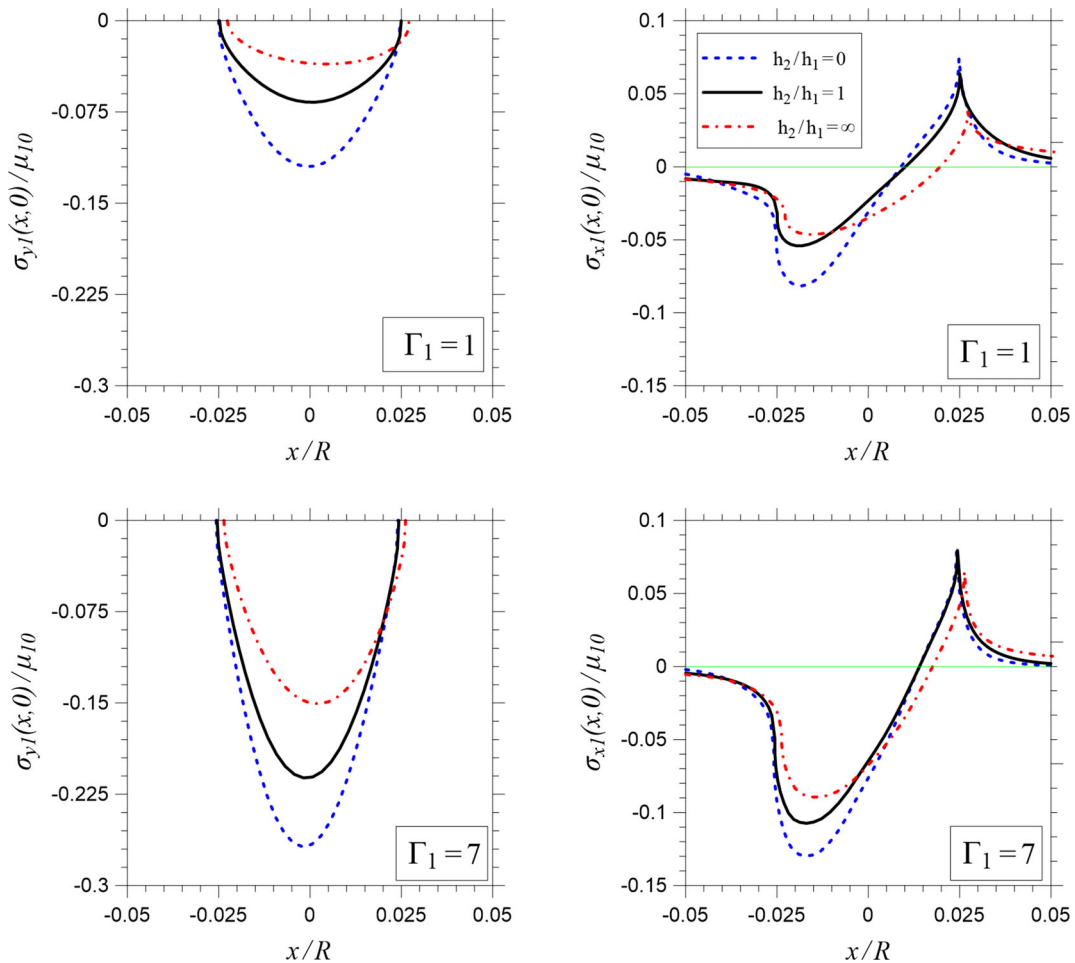


**Fig. 5** Contact stress and in-plane stress distribution for various values of the thickness ratio,  $h_2/h_1, \Gamma_2 = \mu_{22}/\mu_{21} = 1, \Gamma_1 = \mu_{11}/\mu_{10}, \eta = 0.5, R/h_1 = 100, (a + b)/R = 0.05$

case ( $\eta = 0$ ), and Fig. 3c, d is for the frictional case with the friction coefficient  $\eta = 1$ . The effect of stiffening ( $\Gamma_1 > 1$ ) or softening ( $\Gamma_1 < 1$ ) layer 1 on the contact stresses can readily be observed. There is a symmetric behavior on the contact pressure for the frictionless case. The in-plane contact stress,  $\sigma_{x1}(x, 0)$ , has a tensile peak at both ends of the contact for the stiffening layer ( $\Gamma_1 = 7$ ) and the homogeneous layer ( $\Gamma_1 = 1$ ) for the frictionless contact. However, there is no tensile peak for the softening layer ( $\Gamma_1 = 1/7$ ) at the contact ends. The in-plane stress component is important for the fatigue crack propagation issues related to the contact field. Observe that the lowest peak in the in-plane contact stress is observed for the softening layer ( $\Gamma_1 = 1/7$ ) in the case of frictional contact. If Figs. 2b and 3b are compared for the frictionless contact and homogeneous materials ( $\Gamma = 1$ ), one can see that there is no tensile stress on the contact area (Fig. 2b); however, there exist tensile stresses at both ends of the contact for bilayers due to the support effect of the bottom layer (Fig. 3b).

The effect of material property grading for both layers is investigated in detail in Fig. 4. In Fig. 4a and 4b, the effect of stiffness ratio  $\Gamma_2$  is investigated by taking  $\Gamma_2 = 1$  (homogeneous second layer). Again when the stiffness ratio  $\Gamma_2$  is decreased or the layer softens, both contact pressure and in-plane stresses decrease. The stiffness ratio  $\Gamma_2$  has the same effect on the contact stresses as the stiffness ratio  $\Gamma_1$ . However, the effect of  $\Gamma_2$  on the in-plane stresses at the trailing edge of the contact is small when  $\Gamma_1$  is fixed at 7. Note that the tensile peak in in-plane stresses at the trailing edge of the contact decreases for the softening layer  $\Gamma_1 = 1/7$ . In Fig. 4c, d, the effect of the stiffness ratio  $\Gamma_2$  is investigated by taking  $\Gamma_1 = 7$ . When the layer 1 gets stiffer (see for example  $\Gamma_1 = 7$ ), there is a diverse effect on the contact stress levels.

The effect of the thickness ratio on the contact and in-plane stresses is shown in Fig. 5. It is evident that when the thickness of layer 2 is increased or the layer 2 becomes half plane ( $h_2 \rightarrow \infty$ ), the value of the contact

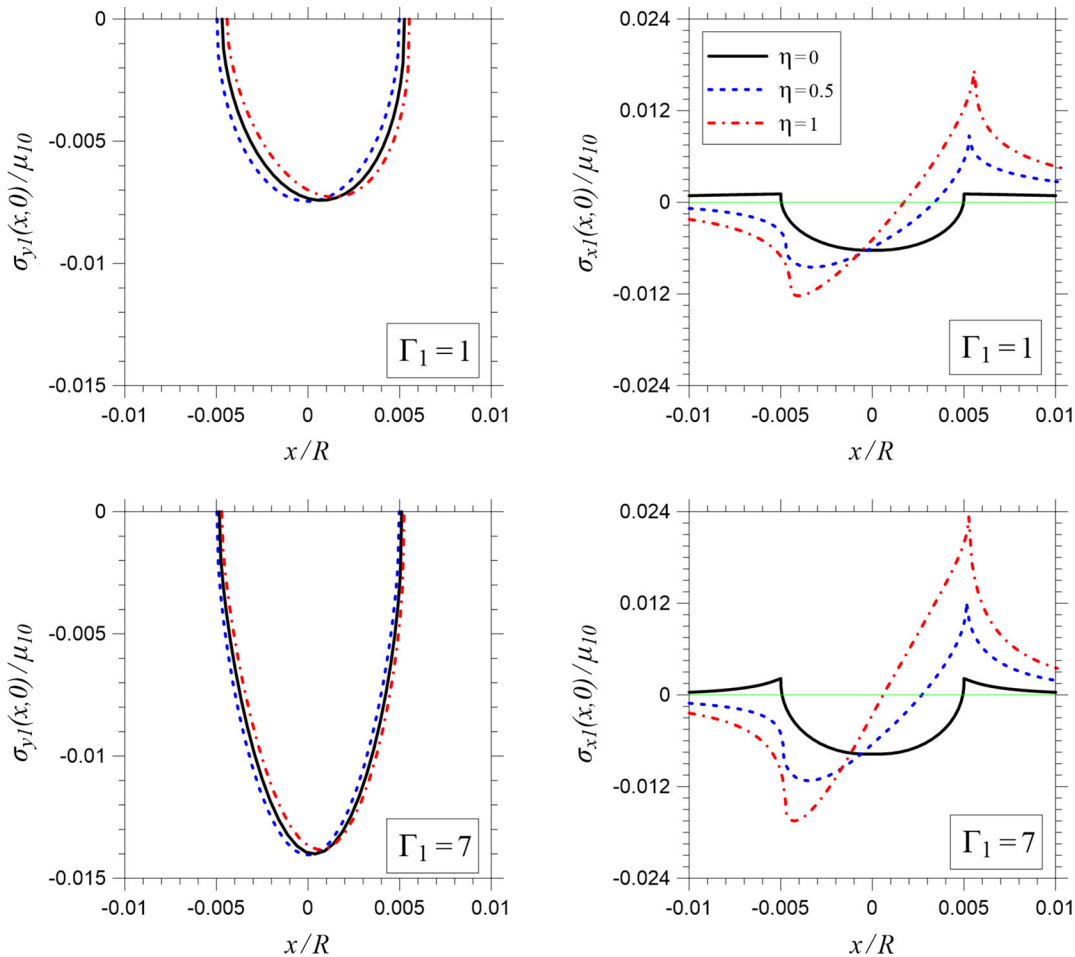


**Fig. 6** Contact stress and in-plane stress distribution for various values of the coefficient of friction,  $\eta$ ,  $\Gamma_2 = \mu_{22}/\mu_{21} = 1$ ,  $\Gamma_1 = \mu_{11}/\mu_{10}$ ,  $R/h_1 = 100$ ,  $(a + b)/R = 0.01$ ,  $h_2/h_1 = 1$

and in-plane stresses decrease due to the support effect. Note that the contact stress values for any  $h_1/h_2$  would be in the range between the contact stress of ( $h_1/h_2 = 0$ ) and ( $h_1/h_2 \rightarrow \infty$ ).

Figure 6 depicts the effect of the coefficient of friction,  $\eta$ , on the contact stress distribution. As the friction coefficient gets larger, the tensile peak increases for the in-plane stresses at the trailing edge.

## 6 Conclusions

The results obtained from this study show that in sliding contact problems for a graded bilayer the influence of not only the coefficient of friction (which is expected) but also the material inhomogeneity constants  $\gamma_1$ ,  $\gamma_2$  as well as stiffness mismatch at the interface on the contact stresses, particularly the in-plane component of the stress state at the surface, can be quite significant.

The most important point of this study is the behavior of in-plane stresses at the trailing edge of the contact for the problems involving friction and at both ends of the contact for the frictionless case. It is seen that the trailing edge of the contact is more prone to contact damage and possible location for surface crack that would lead to fatigue crack initiation and propagation.

For the equivalent values of the external load, the contact areas decrease with increasing stiffness of the layers, increase with increasing height of the lower layer, and become almost the same as in the frictionless case if the friction coefficient increases.

Another important conclusion drawn from this study is that the contact stress behavior at the ends of the contact is completely different as opposed to one layer bonded to a half plane.

## References

- Alinia, Y., Beheshti, A., Guler, M.A., El-Borgi, S., Polycarpou, A.A.: Sliding contact analysis of functionally graded coating/substrate system. *Mech. Mater.* **94**, 142–155. <http://www.sciencedirect.com/science/article/pii/S0167663615002598> (2016)
- Bakirtas, I.: The problem of a rigid punch on a non-homogeneous elastic half space. *Int. J. Eng. Sci.* **18**, 597–610. <http://www.sciencedirect.com/science/article/pii/0020722580901329> (1980)
- Chen, P., Chen, S.: Contact behaviors of a rigid punch and a homogeneous half-space coated with a graded layer. *Acta Mech.* **223**, 563–577 (2012). doi:10.1007/s00707-011-0581-0
- Chen, P., Chen, S., Peng, J.: Frictional contact of a rigid punch on an arbitrarily oriented gradient half-plane. *Acta Mech.* **226**, 4207–4221 (2015). doi:10.1007/s00707-015-1457-5
- Chidlow, S., Teodorescu, M.: Sliding contact problems involving inhomogeneous materials comprising a coating-transition layer-substrate and a rigid punch. *Int. J. Solids Struct.* **51**, 1931–1945. <http://www.sciencedirect.com/science/article/pii/S0020768314000432> (2014)
- Choi, H.J.: On the plane contact problem of a functionally graded elastic layer loaded by a frictional sliding flat punch. *J. Mech. Sci. Technol.* **23**, 2703–2713 (2009). doi:10.1007/s12206-009-0734-4
- Comez, I.: Contact problem of a functionally graded layer resting on a Winkler foundation. *Acta Mech.* **224**, 2833–2843 (2013). doi:10.1007/s00707-013-0903-5
- Comez, I.: Contact problem for a functionally graded layer indented by a moving punch. *Int. J. Mech. Sci.* **100**, 339–344. <http://www.sciencedirect.com/science/article/pii/S0020740315002507> (2015)
- Dag, S., Guler, M.A., Yildirim, B., Ozatag, A.C.: Sliding frictional contact between a rigid punch and a laterally graded elastic medium. *Int. J. Solids Struct.* **46**, 4038–4053. <http://www.sciencedirect.com/science/article/pii/S0020768309002844> (2009)
- Erdogan, F.: *Mixed Boundary Value Problems in Mechanics*, vol. 4. Pergamon Press, Oxford (1978)
- Giannakopoulos, A., Pallot, P.: Two-dimensional contact analysis of elastic graded materials. *J. Mech. Phys. Solids* **48**(8), 1597–1631. <http://www.sciencedirect.com/science/article/pii/S002250969900068X> (2000)
- Giannakopoulos, A., Suresh, S.: Indentation of solids with gradients in elastic properties: part i. Point force. *Int. J. Solids Struct.* **34**, 2357–2392. <http://www.sciencedirect.com/science/article/pii/S0020768396001710> (1997)
- Giannakopoulos, A., Suresh, S.: Indentation of solids with gradients in elastic properties: part ii. Axisymmetric indentors. *Int. J. Solids Struct.* **34**, 2393–2428. <http://www.sciencedirect.com/science/article/pii/S0020768396001722> (1997)
- Guler, M., Erdogan, F.: Contact mechanics of graded coatings. *Int. J. Solids Struct.* **41**, 3865–3889. <http://www.sciencedirect.com/science/article/pii/S0020768304000824> (2004)
- Guler, M., Erdogan, F.: The frictional sliding contact problems of rigid parabolic and cylindrical stamps on graded coatings. *Int. J. Mech. Sci.* **49**, 161–182. <http://www.sciencedirect.com/science/article/pii/S0020740306001913> (2007)
- Guler, M., Ozturk, M., Kucuksucu, A.: The frictional contact problem of a rigid stamp sliding over a graded medium. *Key Eng. Mater.* **681**, 155–174 (2016)
- Ke, L.-L., Wang, Y.-S.: Two-dimensional contact mechanics of functionally graded materials with arbitrary spatial variations of material properties. *Int. J. Solids Struct.* **43**, 5779–5798. <http://www.sciencedirect.com/science/article/pii/S002076830500418X> (2006)
- Ke, L.-L., Wang, Y.-S.: Two-dimensional sliding frictional contact of functionally graded materials. *Eur. J. Mech. A/Solids* **26**, 171–188. <http://www.sciencedirect.com/science/article/pii/S0997753806000519> (2007)

19. Kieback, B., Neubrand, A., Riedel, H.: Processing techniques for functionally graded materials. *Mater. Sci. Eng. A* **362**, 81–106, papers from the German Priority Programme (Functionally Graded Materials). <http://www.sciencedirect.com/science/article/pii/S0921509303005781> (2003)
20. Liu, T.-J., Wang, Y.-S., Zhang, C.: Axisymmetric frictionless contact of functionally graded materials. *Arch. Appl. Mech.* **78**, 267–282 (2008). doi:[10.1007/s00419-007-0160-y](https://doi.org/10.1007/s00419-007-0160-y)
21. Miranda, P., Pajares, A., Guiberteau, F., Cumbreira, F. L., Lawn, B.R., Contact fracture of brittle bilayer coatings on soft substrates. *J. Mater. Res.* **16**, 115–126. [http://journals.cambridge.org/article\\_S0884291400057459](http://journals.cambridge.org/article_S0884291400057459) (2001)
22. Yang, J., Ke, L.-L.: Two-dimensional contact problem for a coating–graded layer–substrate structure under a rigid cylindrical punch. *Int. J. Mech. Sci.* **50**, 985–994. <http://www.sciencedirect.com/science/article/pii/S0020740308000490> (2008)